ISBN: 978-3-95450-184-7 doi:10.18429/JACoW-IPAC2018-THPMK051

THEORETICAL FORMULATION OF IMPROVED SASE FEL BASED ON SLIPPAGE ENHANCEMENT SCHEME*

C.-Y. Tsai[1†], J. Wu[1‡], C. Yang[1,2], M. Yoon[3], and G. Zhou[1,4]
[1]SLAC National Accelerator Laboratory, Menlo Park, California, USA
[2]NSRL, University of Science and Technology of China, Hefei, Anhui, China
[3]Department of Physics, Pohang University of Science and Technology, Pohang, Korea
[4]Institute of High Energy Physics, and UCAS, Chinese Academy of Sciences, Beijing, China

Abstract

A method to improve the spectral brightness of self-amplified spontaneous emission (SASE) based on slippage enhancement has been proposed [1–4]. An implementation is to insert a series of magnetic chicanes to introduce a path-length delay of the electron beam to the radiation beam. By correlating the electron slices of neighboring cooperation distances this can lengthen the collective interaction and thus enhance the spectral brightness. In the existing literature most studies rely on numerical simulations and there is limited work on analytical analysis. In this paper we formulate the problem of slippage enhanced SASE (SeSASE) high-gain FEL with inclusion of by-pass magnetic chicanes. The analysis takes the finite energy spread of the electron beam and the nonzero momentum compaction of the chicane into consideration. The evolution of spectral bandwidth of SeSASE is compared with that of usual SASE in theory. The effects of finite beam energy spread and non-isochronisity are also quantified.

THEORETICAL FORMULATION

In the theoretical formulation we largely follow the notation used in the book by K.-J. Kim *et al*. [5]. Let us start from the single-particle equations of motion

$$\frac{d\theta_j}{dz} = 2k_u\eta_j \tag{1}$$

$$\frac{d\eta_j}{dz} = \chi_1 E(\theta_j; z) + c.c. = \chi_1 \int d\nu E_\nu(z) e^{i\nu\theta_j} + c.c. \tag{2}$$

where θ_j is the ponderomotive phase of j-th particle, $\eta_j = (\gamma_j - \gamma_R)/\gamma_R$ is the energy deviation to the resonance one γ_R, E and E_ν are the electric field in time and normalized frequency domain ($\nu = \omega/\omega_1$), respectively, $\kappa_1 = eK[JJ]/4\epsilon_0\gamma_R$ and $\chi_1 = eK[JJ]/2\gamma_R^2 mc^2$, with K the dimensionless undulator parameter and $[JJ]$ the coupling factor. The 1-D wave equation based on slowly varying envelope approximation can be formulated as

$$\left(\frac{\partial}{\partial z} + k_u \frac{\partial}{\partial\theta}\right) E(\theta; z) = -\kappa_1 n_e \frac{2\pi}{N_\lambda} \sum_{j=1}^{N_e} e^{-i\theta_j(z)} \delta\left[\theta - \theta_j(z)\right] \tag{3}$$

where N_λ is the number of electrons in one radiation wavelength λ_1. The electron phase space distribution can be described using the Klimontovich distribution function to retain the discrete nature of the electrons, $F(\theta, \eta; z) = \frac{k_1}{I/ec} \sum_{j=1}^{N_e} \delta\left[\theta - \theta_j(z)\right] \delta\left[\eta - \eta_j(z)\right]$ in which the dynamics is governed by the continuity equation $\frac{dF}{dz} = \frac{\partial F}{\partial z} + \frac{\partial F}{\partial\theta}\frac{d\theta}{dz} + \frac{\partial F}{\partial\eta}\frac{d\eta}{dz} = 0$. In general the continuity equation is nonlinear since $d\eta/dz$ depends on F as well. In the following analysis, we are interested in the linear regime where the electron phase space distribution can be well separated into the smooth background and the small perturbing part, in which the information of shot noise and perturbation due to FEL process is contained. In addition we make the coasting beam approximation in describing the electron beam distribution. Under this approximation we have neglected the situation when the radiation field slips over the edge of an electron bunch, i.e., the slippage-induced superradiance FEL [6] is excluded in our analysis. After linearizing the continuity equation and transforming to the normalized frequency domain, we obtain

$$\left(\frac{\partial}{\partial z} + 2i\nu k_u \eta\right) F_\nu(\eta; z) + \chi_1 E_\nu(z) \frac{dV}{d\eta} = 0 \tag{4}$$

where $V(\eta)$ the electron beam energy distribution. The wave equation Eq. (3) represented in the frequency domain is

$$\left(\frac{\partial}{\partial z} + i\Delta\nu k_u\right) E_\nu(z) = -\kappa_1 n_e \int d\eta F_\nu(\eta; z) \tag{5}$$

Here we note that Eqs. (4) and (5) are more general and can be reduced to those based on Bonifacio *et al*. collective-variable description in the cold-beam limit [7]. To solve Eqs. (4) and (5) as an initial value problem, we shall employ Laplace transform and the resultant electric field in the frequency domain can be expressed as

$$E_\nu(z) = \oint \frac{e^{-i\mu 2\rho k_u z}}{2\pi i D(\mu)} \left[E_\nu(0) + \frac{i\kappa_1 n_e}{2\rho k_u} \frac{1}{N_\lambda} \sum_{j=1}^{N_e} \frac{e^{-i\nu\theta_j(0)}}{\eta_j(0)/\rho - \mu}\right] d\mu \tag{6}$$

where the dispersion relation $D(\mu) = \mu - \frac{\Delta\nu}{2\rho} - \int \frac{V(\eta) d\eta}{\eta/\rho - \mu} = 0$. ρ is the FEL or Pierce parameter. The contour integral should enclose all the singularities and draw in the lower complex-μ plane. The electron phase space distribution can be obtained $F_{\nu,\mu}(\eta) = \frac{i\chi_1}{2\rho k_u} \frac{dV/d\eta}{\eta/\rho - \mu} E_{\nu,\mu}$, provided $E_{\nu,\mu}$ is given.

---

* The work was supported by the US Department of Energy (DOE) under contract DE-AC02-76SF00515 and the US DOE Office of Science Early Career Research Program grant FWP-2013-SLAC-100164.
† jcytsai@SLAC.Stanford.EDU
‡ jhwu@SLAC.Stanford.EDU

ISBN: 978-3-95450-184-7 doi:10.18429/JACoW-IPAC2018-THPMK051

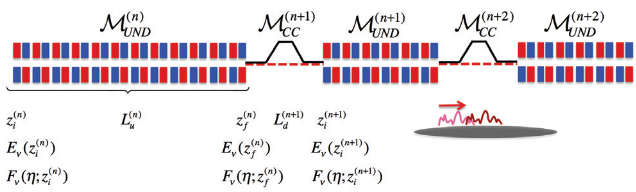

Figure 1: Schematic layout of multi-stage SeSASE FEL.

Now we consider the SeSASE FEL process with a schematic layout shown in Fig. 1. Hereafter we assume the chicane(s) shall be placed where the FEL process is dominated by the unstable root, say, μ_3 of $D(\mu)$. This situation corresponds to that occurs after about two FEL gain lengths. In what follows we aim to derive the matrix representation for transport of E_ν and F_ν through undulator section and magnetic chicane. The electric field at the exit of n-th undulator section can be expressed as $E_\nu(z_f^{(n)}) \approx \frac{e^{-i\mu_3 2\rho k_u L_u^{(n)}}}{D'(\mu_3)}\left[E_\nu(z_i^{(n)}) + \frac{i\kappa_1 n_e}{2\rho k_u}\int d\eta \frac{F_\nu(\eta;z_i^{(n)})}{\eta/\rho-\mu_3}\right]$ and the corresponding electron phase space distribution $F_\nu(\eta;z_f^{(n)}) = \frac{i\chi_1}{2\rho k_u}\frac{dV/d\eta}{\eta/\rho-\mu_3}E_\nu(z_f^{(n)})$. After the chicane, the electron beam is bypassed and the electric field acquires an additional phase. The resultant electric field and the electron phase space distribution become $E_\nu(z_i^{(n+1)}) = E_\nu(z_f^{(n)})e^{i\Delta\nu k_u L_d^{(n+1)}} = E_\nu(z_f^{(n)})e^{i\Delta\nu\phi^{(n+1)}}$ and $F_\nu(\eta;z_i^{(n+1)}) = F_\nu(\eta;z_f^{(n)})e^{i\Delta\theta^{(n+1)}(\eta)}$, respectively. In a general bypass transport line, we have $\Delta\theta^{(n+1)}(\eta) = k_r R_{56}^{(n+1)}\eta - \psi^{(n+1)}$ and $\psi^{(n+1)} = k_r R_{56}^{(n+1)}\big/2$ with R_{56} the momentum compaction. In terms of matrix representation, we have $\begin{bmatrix}E_\nu\\F_\nu\end{bmatrix}_f^{(n)} = \frac{G}{D'(\mu_3)}\mathcal{M}_{\text{UND}}^{(n)}\begin{bmatrix}E_\nu\\F_\nu\end{bmatrix}_i^{(n)} = \frac{G}{D'(\mu_3)}\begin{pmatrix}1 & \xi_2\mathcal{H}\\ \frac{\xi_1 V'}{\eta/\rho-\mu_3} & \frac{\xi_1 V'\xi_2\mathcal{H}}{\eta/\rho-\mu_3}\end{pmatrix}\begin{bmatrix}E_\nu\\F_\nu\end{bmatrix}_i^{(n)}$ for the undulator segment, where $G^{(n)} \equiv e^{-i2\mu_3\rho k_u L_u^{(n)}}, G^{(n+1)}G^{(n)} = e^{-i2\mu_3\rho k_u\left(L_u^{(n+1)}+L_u^{(n)}\right)}, \xi_1 \equiv i\chi_1/2\rho k_u, \xi_2 \equiv i\kappa_1 n_e/2\rho k_u, \xi_1\xi_2 = -\rho$, and $\mathcal{H}(\ldots) \equiv \int\frac{(\ldots)d\eta}{\eta/\rho-\mu_3}$. Furthermore, we have $\begin{bmatrix}E_\nu\\F_\nu\end{bmatrix}_i^{(n+1)} = \mathcal{M}_{\text{CC}}^{(n+1)}\begin{bmatrix}E_\nu\\F_\nu\end{bmatrix}_f^{(n)} = \begin{pmatrix}e^{i\Delta\nu\phi^{(n+1)}} & 0\\ 0 & e^{i\Delta\theta^{(n+1)}}\end{pmatrix}\begin{bmatrix}E_\nu\\F_\nu\end{bmatrix}_f^{(n)}$ for the by-pass chicane. Now, let us consider the 1/2 undulator-chicane-1/2 undulator module (Fig. 1). The resultant expression at the exit of this module is

$$\begin{bmatrix}E_\nu\\F_\nu\end{bmatrix}_f^{(2)} = \frac{G^{(2)}G^{(1)}}{D'(\mu_3)}\mathcal{M}_{\text{UND}}^{(2)}\mathcal{M}_{\text{CC}}\mathcal{M}_{\text{UND}}^{(1)}\begin{bmatrix}E_\nu\\F_\nu\end{bmatrix}_i^{(1)} \tag{7}$$

where the matrix multiplication can be analytically obtained.

Note that $\mathcal{H}$ depends on the specific energy distribution of electron beam. For the cold-beam case, we have

$$\mathcal{H}\left(e^{i\Delta\theta}\frac{\xi_1 V'}{\eta/\rho-\mu_3}\right)_{\text{cold}} = -\xi_1\left(\frac{ik_r R_{56}e^{-i\psi}}{\mu_3^2} + \frac{2}{\rho}\frac{e^{-i\psi}}{\mu_3^3}\right) \tag{8}$$

and for the uniform energy distribution we have

$$\mathcal{H}\left(e^{i\Delta\theta}\frac{\xi_1 V'}{\eta/\rho-\mu_3}\right)_{\text{uniform}} = -\frac{\xi_1}{\rho\zeta}\left(\frac{e^{-i\left(\psi-k_r R_{56}\rho\zeta/2\right)}}{\left(\zeta/2-\mu_3\right)^2} - \frac{e^{-i\left(\psi+k_r R_{56}\rho\zeta/2\right)}}{\left(\zeta/2+\mu_3\right)^2}\right) \tag{9}$$

where $V(\eta) = \frac{1}{\rho\zeta}$, $|\eta| \leqslant \frac{\rho\zeta}{2}$ and 0 elsewhere. Figure 2 illustrates the imaginary part of (unstable) root of $D(\mu)$ and $\mathcal{H}$ for the case of uniform energy distribution.

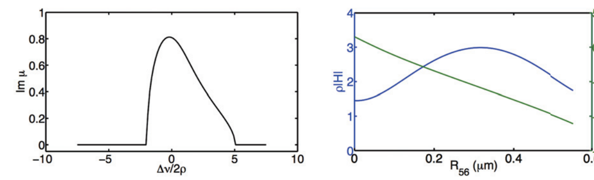

Figure 2: (Left) The growth rate as a function of scaled detuning. (Right) $|\mathcal{H}|$ and Φ as a function of R_{56}, where $\mathcal{H} \equiv \xi_1|H|e^{i\Phi}$. Here $\Delta\nu = 0.4\rho, \Delta\eta = 5\times10^{-4}, \zeta = 0.89$.

For simplicity in what follows we define $\mathcal{H}\left(e^{i\Delta\theta^{(n)}}\frac{\xi_1 V'}{\eta/\rho-\mu_3}\right) \equiv \xi_1 H^{(n)}$. Assume the individual undulator segments are identical. For N undulator sections

$$\begin{bmatrix}E_\nu\\F_\nu\end{bmatrix}_f^{(N)} = \frac{G^{(N)}}{D'(\mu_3)}\prod_{j=2}^{N}G^{(j)}\left(e^{i\Delta\nu\phi^{(j)}} - \rho H^{(j)}\right)\mathcal{M}_{\text{UND}}\begin{bmatrix}E_\nu\\F_\nu\end{bmatrix}_i^{(1)} \tag{10}$$

Here we note that Eq. (10) is a general expression, from which we will evaluate the SeSASE performance, its spectral and statistical properties. These include the spectral power and bandwidth, the correlation function and coherence length, and can indicate the interference phenomenon. For temporal field profile, we take the inverse Fourier transformration $E_x(z,t) = \int d\nu E_\nu(z)e^{i\Delta\nu[(k_1+k_u)z-\omega_1 t]+i(k_1 z-\omega_1 t)}$. Then for SeSASE case the resultant expression can be obtained

$$E_x^{\text{SeSASE}}(z,t) \propto \frac{e^{\sqrt{3}\rho k_u z}}{\sqrt{z}}\times \left\{\begin{array}{l}\sum_{j=1}^{N_e}e^{-i\omega_1[t-t_j(0)-z/c]-\left[\left(1+i\sqrt{3}\right)/4\sigma_{\tau0}^2\right][t-t_j(0)-z/v_g+\phi]^2}\\ -\rho H\sum_{j=1}^{N_e}e^{-i\omega_1[t-t_j(0)-z/c]-\left[\left(1+i\sqrt{3}\right)/4\sigma_{\tau0}^2\right][t-t_j(0)-z/v_g]^2}\end{array}\right\} \tag{11}$$

In obtaining Eq. (11) we have assumed the weak dependence of H on $\Delta\nu$, so that H is excluded in the integration. The two-wave interference is obvious in the expression: the first term corresponds to the original wave packet and the second term indicates the newly grown wave packet.

Let us evaluate the power spectral density for SASE [5],

$$\left.\frac{dP}{d\omega}\right|_{\text{SASE}} \approx e^{z/L_G-(\omega-\omega_m)^2/2\omega_m^2\sigma_{\nu0}^2}g_A\left(\left.\frac{dP}{d\omega}\right|_0 + g_S\frac{\rho\gamma_R mc^2}{2\pi}\right) \tag{12}$$

where $g_A = \frac{1}{|D'(\mu)|^2}$ and $g_S = \int\frac{V(\eta)d\eta}{|\eta/\rho-\mu|^2}$. Here g_A measures how the initial radiation power and shot noise seed the interaction, while g_S quantifies the relative increase in shot noise seeding as the beam energy spread increases [5].

ISBN: 978-3-95450-184-7 doi:10.18429/JACoW-IPAC2018-THPMK051

Now we consider the simplest SeSASE case, i.e., $N = 2$. Then we have $E^{\text{SeSASE}}_{\nu,f} = (e^{i\Delta\nu\phi} - \rho H)\, E^{\text{SASE}}_{\nu,f}$. The power spectral density can be expressed as $\frac{dP}{d\omega}\big|_{\text{SeSASE}} = \mathcal{S}(\phi, H)\, \frac{dP}{d\omega}\big|_{\text{SASE}}$, where $\mathcal{S}(\phi, H) = 1 + \rho^2|H|^2 - 2\rho\,|H|\cos(\Delta\nu\phi + \Phi)$. Here we note that the shape function $\mathcal{S}$ is general in the sense that it contains the finite energy spread of the electron beam and allows the nonzero R_{56}. The spectrum bandwidth can then be evaluated analytically by $\sigma_\nu^2 \equiv \int d\nu \nu^2 dP/d\nu \Big/ \int d\nu dP/d\nu$

$$\frac{\sigma_\nu}{\nu_m\sigma_{\nu0}} = \sqrt{\frac{1 + \rho^2|H|^2 - 2\rho\,|H|\,(1 - \nu_m^2\sigma_{\nu0}^2\phi^2)\cos(\Delta\nu_m\phi + \Phi)e^{-\nu_m^2\sigma_{\nu0}^2\phi^2/2}}{1 + \rho^2|H|^2 - 2\rho\,|H|\cos(\Delta\nu_m\phi + \Phi)e^{-\nu_m^2\sigma_{\nu0}^2\phi^2/2}}} \tag{13}$$

Figure 3 shows the shape function as a function of R_{56} for several different frequency detunes and the spectrum bandwidth of SeSASE as a function of phase shift ϕ for $N = 2$ case. In the numerical illustration we assume $\lambda_1 = 0.31$ nm, $\rho = 5.6 \times 10^{-4}$, the full-width (uniform) energy spread 5×10^{-4}, and the 1-D gain length $L_G = 2.13$ m.

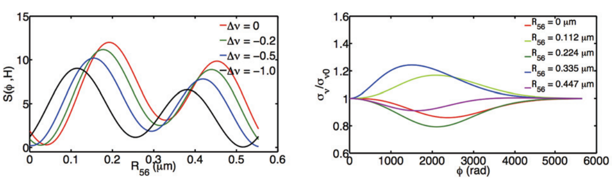

Figure 3: (Left) The shape function $\mathcal{S}$ as a function of momentum compaction R_{56} for different $\Delta\nu$. (Right) The relative frequency bandwidth as a function of phase shift ϕ for different R_{56} at $z = 10L_G$.

Similarly, for the case of $N = 3$, we have $E^{\text{SeSASE}}_{\nu,f} = (e^{i\Delta\nu\phi_{(3)}} - \rho H^{(3)})\,(e^{i\Delta\nu\phi_{(2)}} - \rho H^{(2)})\, E^{\text{SASE}}_{\nu,f}$ and the power spectral density $\frac{dP}{d\omega}\big|_{\text{SeSASE}} = \mathcal{S}(\phi_{(2)}, \phi_{(3)}, H^{(2)}, H^{(3)})\, \frac{dP}{d\omega}\big|_{\text{SASE}}$. The spectrum bandwidth can also be obtained analytically.

In the most general case, the shape function can be symbolically formulated as $\left|E^{\text{SeSASE}}_{\nu,f}\right|^2 = \left|\prod_{j=2}^{N}\left(e^{i\Delta\nu\phi^{(j)}} - \rho H^{(j)}\right)\right|^2 \left|E^{\text{SASE}}_{\nu,f}\right|^2$. Having evaluated the spectral shape characteristics, let us look at the correlation function, expressed as $C(\tau) \equiv \left\langle \int dt E(t)E^*(t+\tau)\right\rangle \Big/ \left\langle \int dt |E(t)|^2\right\rangle = \left\langle \int d\omega \frac{dP}{d\omega} e^{-i\omega\tau}\right\rangle \Big/ \langle P\rangle$, where the Weiner-Khinchin theorem has been used in the second equality [5]. The denominator can be obtained by $\langle P\rangle = \left\langle \int d\nu \frac{dP}{d\nu}\right\rangle$ where $dP/d\nu$ for SASE is given in Eq. (12) $\langle P\rangle_{\text{SASE}} = g_A g_S \frac{\rho\gamma_R mc^2}{2\pi}\sqrt{2\pi}\omega_1\sigma_{\nu0}e^{z/L_G}$. For SeSASE case, we have

$$\langle P\rangle_{\text{SeSASE}} = \langle P\rangle_{\text{SASE}}\left[1 + \rho^2|H|^2 - 2\rho\,|H|\,e^{-\sigma_{\nu0}^2\phi^2/2}\cos\Phi\right]. \tag{14}$$

In the $C(\tau)$ expression the numerator for SASE case can be evaluated to be $\left\langle \int d\omega \frac{dP}{d\omega} e^{-i\omega\tau}\right\rangle_{\text{SASE}} = g_A g_S \frac{\rho\gamma_R mc^2}{2\pi}\sqrt{2\pi}\omega_1\sigma_{\nu0}e^{z/L_G}e^{-\omega_1^2\sigma_{\nu0}^2\tau^2/2}$ and for SeSASE case

$$\left\langle \int d\omega \frac{dP}{d\omega} e^{-i\omega\tau}\right\rangle_{\text{SeSASE}} = \left\langle \int d\omega \frac{dP}{d\omega} e^{-i\omega\tau}\right\rangle_{\text{SASE}} \times \begin{Bmatrix} 1 + \rho^2|H|^2 - \\ \rho\,|H|\,e^{-\sigma_{\nu0}^2\phi^2/2}\left(e^{i\Phi - \sigma_{\nu0}^2(\omega_1\tau - \phi)^2/2} + e^{-i\Phi - \sigma_{\nu0}^2(\omega_1\tau + \phi)^2/2}\right)\end{Bmatrix} \tag{15}$$

The correlation function can now be derived $C(\tau)_{\text{SASE}} = e^{-\omega_m^2\sigma_{\nu0}^2\tau^2/2}$ for SASE case, and for SeSASE case shown in Eq. (16) below. The correlation or coherence time, defined as $t_{\text{coh}} \equiv \int d\tau |C(\tau)|^2$, can also be computed $t^{\text{SASE}}_{\text{coh}} = \frac{\sqrt{\pi}}{\omega_1\sigma_{\nu0}}$ for SASE case and for SeSASE case shown in Eq. (17). Here we remark that the result for SASE case is similar to the property of the chaotic light while there is an additional factor for SeSASE case.

$$C(\tau)_{\text{SeSASE}} = C(\tau)_{\text{SASE}}\left[\frac{1 + \rho^2|H|^2 - \rho\,|H|\,e^{-\sigma_{\nu0}^2\phi^2/2}\left(e^{i\Phi - \sigma_{\nu0}^2(\omega_1\tau - \phi)^2/2} + e^{-i\Phi - \sigma_{\nu0}^2(\omega_1\tau + \phi)^2/2}\right)}{1 + \rho^2|H|^2 - 2\rho\,|H|\,e^{-\sigma_{\nu0}^2\phi^2/2}\cos\Phi}\right] \tag{16}$$

$$t^{\text{SeSASE}}_{\text{coh}} = t^{\text{SASE}}_{\text{coh}}\left\{\frac{\left(1 + \rho^2|H|^2\right)^2 - 4\rho\,|H|\left(1 + \rho^2|H|^2\right)e^{-\sigma_{\nu0}^2\phi^2/4}\cos\Phi + 2\rho^2|H|^2\left(1 + e^{-\sigma_{\nu0}^2\phi^2}\cos 2\Phi\right)}{\left(1 + \rho^2|H|^2 - 2\rho\,|H|\,e^{-\sigma_{\nu0}^2\phi^2/2}\cos\Phi\right)^2}\right\} \tag{17}$$

SUMMARY AND OUTLOOK

In this paper we have formulated the slippage enhanced SASE (SeSASE) high-gain FEL process with inclusion of by-pass magnetic chicanes and extension to a general N undulator-chicane moduli. The analysis takes the finite energy spread of the electron beam and the nonzero momentum compaction of the chicane into consideration. The evolution of spectral bandwidth of SeSASE is derived and expressed in a combined form with that of usual SASE case. The effects of finite beam energy spread and non-isochronicity are also explicitly expressed. These analytical expressions may be used to improve or optimize the SeSASE performance. Further investigation on improving the SeSASE performance with varying bunch current density is ongoing.

REFERENCES

[1] J. Wu *et al.*, "Generation of Longitudinally Coherent Ultra High Power X-Ray FEL Pulses by Phase and Amplitude Mix-

ISBN: 978-3-95450-184-7 doi:10.18429/JACoW-IPAC2018-THPMK051

ing", in *Proc. FEL'12*, Nara, Japan, Aug. 2012, paper TUPD07.

[2] J. Wu *et al.*, "X-ray Spectra and Peak Power Control with SeSASE", in *Proc IPAC'13*, Shanghai, China, May 2013, paper WEODB101.

[3] J. Wu *et al.*, "Slippage-Enhanced SASE FEL", in *Proc. FEL'17*, Santa Fe, USA, Aug. 2017, paper TUP058.

[4] B. W. J. McNeil *et al.*, "Transform-Limited X-Ray Pulse Generation from a High-Brightness Self-Amplified Spontaneous-Emission Free-Electron Laser", *PRL*, vol. 110, p. 134802, 2013.

[5] K.-J. Kim, Z. Huang, and R. Lindberg, *Synchrotron radiation and free-electron lasers: Principles of coherent x-ray generation*, Cambridge University Press, 2017.

[6] R. Bonifacio and B.W.J. McNeil, "Slippage and superradiance in the high-gain FEL", *NIMA*, vol. 272, pp. 280-288, 1988.

[7] R. Bonifacio, C. Pellegrini, and L.M. Narducci, "Collective instabilities and high-gain regime in a free electron laser", *Opt. Comm.*, vol. 50, pp. 373-378, 1984.